

A Novel Wave Front Method used for tracking terrestrial concentrator focal spot location.

Joseph N. Beasley
USAF/AFRL/PRSO

Abstract

This paper presents a new sensing method for tracking terrestrial concentrator focal spot location. The new method utilizes the shape and mirror-like surfaces of the absorber as a wave front sensor. The paper begins with a discussion of wave front sensing and how it can be used in optical systems to measure phase differences in light waves across an aperture. The wave front sensing method is then modified from an aperture or lens system into a mirror system. After the method was developed for mirrors, it was developed into a method of detecting focal spot location errors.

Introduction:

Focal control for solar light concentrators is very important. Proper tracking of the sun or proper positioning of the focal spot ensures maximum energy transfer to the fluid being heated. To properly track the sun for maximum heat transfer, the controller requires a sensor with enough resolution to ensure proper control or better optimal control for maximum heat transfer. This paper describes a new sensor to be used for concentrator control. The sensor is shaped like a cone and serves not only as the sensor but also as the solar heat absorber. The method of determining where the focal spot is located on the sensor uses a method derived from a Shack-Hartmann optical wave front sensor.

Wave Front Sensor:

The Hartmann wave front sensor was developed by Hartmann in 1900 and was used for checking optical telescopes for aberrations. It was an array of holes in a plate placed in front of the mirror of the telescope being checked so that light tubes from the array would impinge on the telescope mirror. Two photographic plates were used to collect the light information. One plate was placed just before the focal spot of the telescope and the other one was placed just behind the focal spot. The distance between the plates was chosen so that the light rays would

be separated from each other. The path of the light rays was traceable by measuring the centroids of the two images. Thus, Hartmann was able to determine figures of merit for various large telescopes.¹

Dr. Roland Shack developed the method of replacing the holes of the Hartmann sensor with small lenses or lenslets to improve the capability of the Hartmann sensor when taking images of satellites or stars at the same time as the Wavefront phase error was being determined. The method was developed while solving a problem with imaging satellites and stars from the earth. Dr. Aden Mienel's solution was to determine the Optical Transfer Function of the atmosphere at the same time as the image being taken. The Hartmann sensor was not satisfactory as Mienel could not allow the array to cover the aperture of the telescope because it would eliminate the image of the satellite in favor of determining Wavefront tilt over the imaging of the satellites. Mienel tried to use a beam splitter to take Hartmann images while taking images of the satellites and stars. This method suffered from the weak intensity images of the light rays in the Hartmann sensor. Shack suggested that replacing the apertures in the Hartmann sensor with lenses would eliminate the problems that Mienel was having with his Hartmann device. The lenslets focused spots onto an image plane such that the displacement of the spots from the ideal position of the spots indicated Wavefront tilt.² Thus, the Shack-Hartmann system overcame the shortcomings of the Hartmann sensor while increasing the sensitivities of the Hartmann device alone. A comparison of the two systems is depicted in Figure 1. The Shack-Hartmann sensor is not suitable for use in tracking the focal spot of concentrated solar rays because of the high temperatures encountered in a concentrated sunlight application.

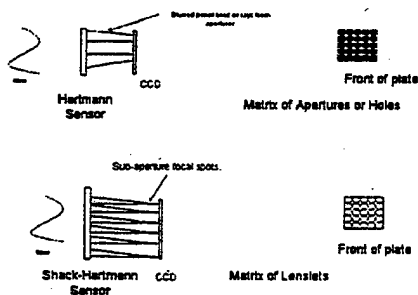


Figure 1 Comparison of Shack-Hartmann and Hartmann Sensor

Cylindrical Mirrors:

Since the sensor for this application uses coiled tubing as its primary configuration, a brief review of cylindrical mirrors is necessary to understand the reflections generated by the conical tubing absorber. Figure 2 shows the normal situation encountered with the use of a cylindrical mirror. In general a cylindrical mirror will tend to compress an object's reflection along the length of the mirror. An object's reflection also tends to get larger as the object moves towards the mirror.

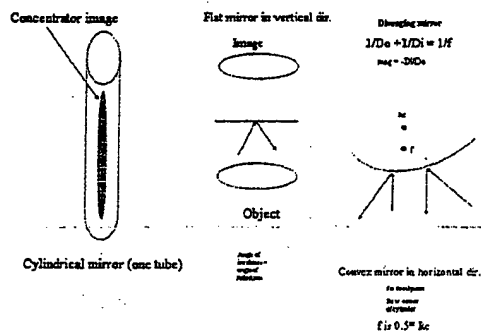


Figure 2 Cylindrical Mirror

Figure 2 also shows the reflections from the cylindrical mirror along two of its axes. In one axis, in the straight on view, the cylindrical mirror acts like a flat mirror with the light rays adhering to the rules for a flat mirror. That is, incident light is reflected such that the reflected ray returns from the mirror as if it originated at a point behind the mirror, at equal distances to the object; this is also a virtual image. Or the reflection occurs such that the reflected ray's angle is equal to the angle of the incident ray. On the other axis of the mirror, reflections follow the rules of a convex mirror. That is, the mirror surface has a virtual focus point and all of the reflected light rays appear to come from that focus point behind the mirror surface. Reflections from other portions of the cylindrical mirror are more complex than the reflections just discussed, however, the overall effect is that the reflection in the cylindrical mirror is compressed along its main axis and appears larger as the viewer moves closer to the mirror.

The new sensor to be described in this paper combines the effects of the cylindrical mirror and the Wavefront sensor to allow tracking of the solar focal spot on the absorber.

Sensor Description:

The sensor being developed for this paper consists of a conical shaped absorber made from one quarter inch ($\frac{1}{4}$ ") metal tubing. For actual application, the tubing would be made from a high temperature metal such as Rhenium or Tungsten. The lens or optic system positions the CCD array to a virtual focal spot location behind the conical absorber. The tubes from the conical absorber act like cylindrical mirrors (torroidal mirrors) in reflecting the sunlight to the CCD. The virtual location is important in applying the principles from wave front sensing, since the wave front sensor uses either apertures or lenslets projected onto the CCD array. The lens system then virtually or mathematically positions the array behind the absorber in a manner similar to the Shack-Hartmann system. The major difference between the method being presented in this paper and the Shack-Hartmann system is that the new sensor tries to maximize the number of wave fronts to determine focal spot location, whereas, the Shack-Hartmann system is normally used to optimize one particular wave front.

Algorithm:

Each image taken would be processed by utilizing profile information along diagonal lines representing the four quadrants of the circle. (Along the 45 degree angles, say) The areas of maximum intensity would be determined along each profile line. The maximums should occur roughly where the tubes appear in the image as they act like cylindrical mirrors. The difference or gradient between these areas should give an indication of the direction to the focal spot. (Almost a centroiding operation on the maximum areas in the image)

By knowing where the center of the absorber is located with respect to the camera (a non-trivial assumption as the camera would probably be mounted to one of the concentrator's movable struts), the computer should be able to generate x, y, z, roll, pitch, and yaw commands for the hexapod controller to move the concentrator to a new position to provide better focus and thus better heating. Figure XX2' shows the schematic of the proposed sensor solution.

Schematic of Proposed Solution

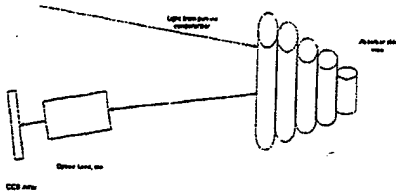


Figure 3 Schematic of Sensor and Camera

For the development of the method presented in this paper, stainless steel $\frac{1}{4}$ inch tubes and a can with a reflective Mylar wrap were used for preliminary imaging, while a copper conical absorber with water-cooling will be used for refinement of the method. Figure 4 shows the stainless steel tubes and Figure 5 presents the water-cooled conical shaped absorber as shown in the schematic in Figure 3. The fluid to be heated is flowed through the absorber tubing and heated by the concentrated light.

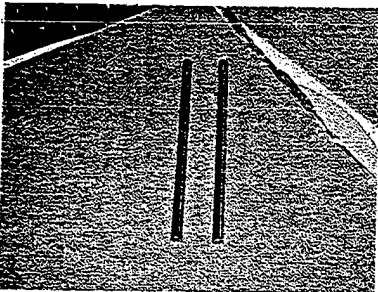


Figure 4 Stainless Steel Tubes

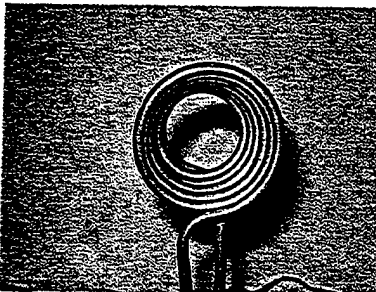


Figure 5 Conical Absorber Sensor

Calculations:

Ray tracing using vectors was used to determine whether the image of the 7-inch diameter concentrator model would reflect off of the tubes and into the aperture of the.

CCD camera. Figure 6 illustrates the situation and the equation shown could be used in an iteration to find the angular extremes that would in fact be imaged in the CCD camera. The figure indicates a theta angle that would in fact be double the angle with respect to the normal vector at the surface of the cylinder. This is happening because of the way things were drawn in Figure 6 and the Law of Reflection: the angle of incidence is equal to the angle of reflection. A quick calculation using just the rays from the extremes of the concentrator model using the Law of Reflection showed that the CCD matrix or camera was able to view all of the reflection of the concentrator model from the tubes.

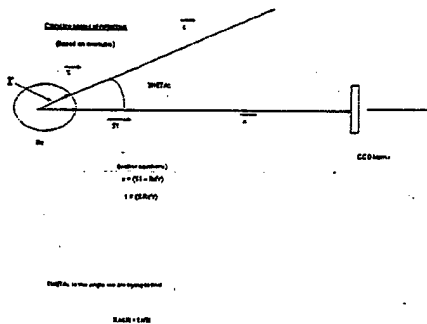


Figure 6 Vector Calculation for Reflection into CCD

The field of view of the CCD camera was determined to be 1.4 (495 rows) X 2 (657 columns) inches at a distance of 1 meter from the tubes and can.

Experimental Setup:

A schematic of the experimental set is shown in Figure 7 and a photo of the experimental equipment is shown in Figure 8.

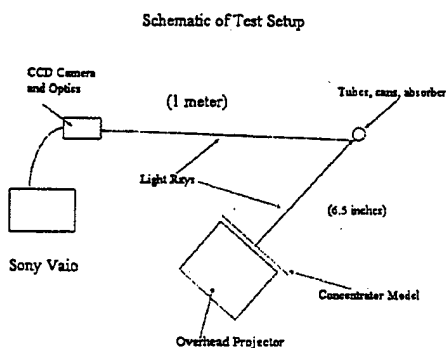


Figure 7 Schematic of Test Setup

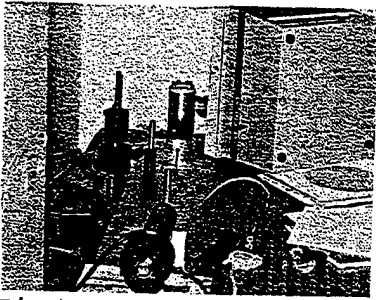


Figure 8 Photo of Test Setup

The CCD camera used was an ST237 CCD camera manufactured by Santa Barbara Instrument Group. A 657 by 495 CCD matrix with 7.4-micrometer pixels characterizes the ST237 CCD camera. A very small aperture, to gain depth of field and a 100 mm lens form the optics for the camera. For the experiments discussed in this paper it is focused for objects located one meter away from the lens.

The concentrator model was generated in Power point and consisted of a 7-inch diagonal circle of white surrounded by a black mask. At the distances shown in Figure 7, the concentrator half-angle model was approximately 7 inches in diameter. A standard overhead projector was used to supply light to the concentrator model using a back projection method.

Images of the stainless steel tubes and the can were taken to discern whether an image of the full view concentrator model could be viewed in the tube. Several different exposure times were used as well as different concentrator patterns from full white circles to circles with varying amounts of area blackened to represent various stages of misalignment. The experiment proceeded by first using one vertical tube, then two vertical tubes and finally a can with reflective Mylar wrapped around the can. The can was approximately 2 inches in diameter and was used to check whether the full images of the concentrator model could be seen by the Camera because the can formed a larger image. The three patterns used are shown in Figures 9 through 11. Figure 9 shows the full concentrator pattern, figure 10 shows pattern one representing a concentrator configuration that would be considered not on focus, and figure 11 shows pattern number 2 with even less white in the concentrator area representing less focus than pattern 1.

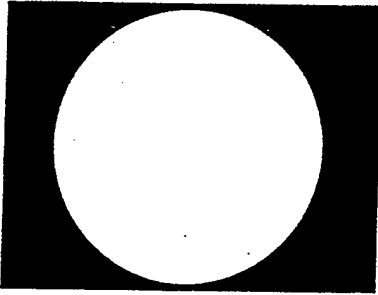


Figure 9 Full Concentrator Model

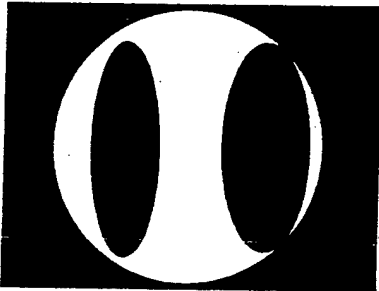


Figure 10 Pattern One Concentrator Model

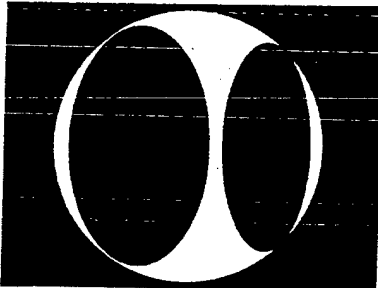


Figure 11 Pattern 2 Concentrator Model

Results:

One tube:

The single tube images indicated that our camera might not have enough resolution to be able to discern between concentrator pattern images. Figure 13 shows the image of one tube with the full concentrator pattern, and figure 14 shows the profile through the image. The images and profiles of the images indicated very little differences between the patterns. The single tube experiment was supposed to show a complete, although distorted image of the concentrator light. At the resolution of the camera, 7.4um pixels focused at 1 meter away from the cylinder did not allow a complete picture of the concentrator model. This experiment may need to be repeated after a camera with higher resolution is acquired.

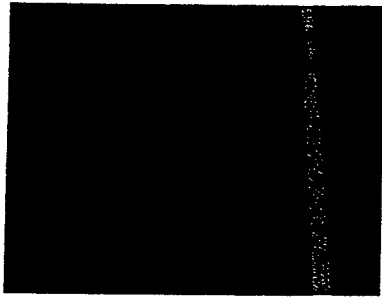


Figure 13 One tube, Full Concentrator

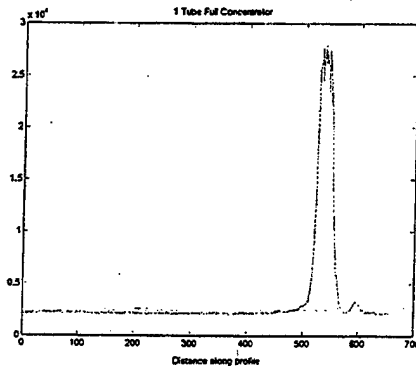


Figure 14 Profile for One Tube Full Concentrator

Can:

The can image is shown in figure 12 and was used to see if the concentrator reflection could be seen using a cylindrical mirror quite a bit larger than the $\frac{1}{4}$ -inch tubes used for the absorber. Although the figure shows a significant bright area on the can, the actual pattern of the concentrator model cannot be discerned. The problem in this instance could be a lack of sufficient Field of View or the problem could be that the camera was not quite focused for the location of the front surface of the can. In either case, an actual pattern could not be made out in the image and nothing more was done with the image. This experiment may be conducted again when a higher resolution camera is obtained.

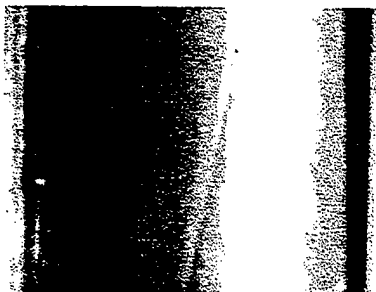


Figure 12 Can with Full Concentrator

Two tube:

The images from the two-tube experiment are shown in Figures 15-17 and their profiles are shown in Figures 18-20. When each pattern's image and profile are examined, the profiles showed a distinct lowering of the peak intensities seen at each tube location. Pattern number 2 showed the smallest peaks compared to the full concentrator model and to pattern number 1. Since pattern 2 had more black area in the white concentrator area, it was expected to produce less intensity on the tubes. These results indicated that the concept of the new sensor would work as thought. However, since the patterns were not directly related to actual misalignment of the concentrator, no actual position information could be derived from the profile information.

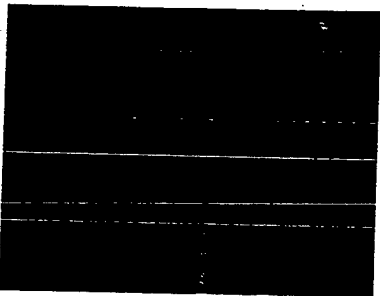


Figure 15 Two Tubes, Full Concentrator

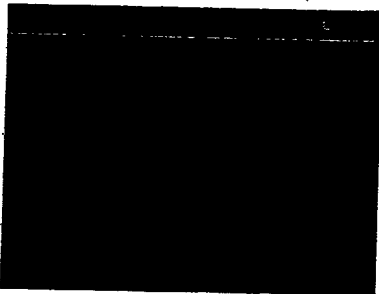


Figure 16 Two Tubes, Pattern 1

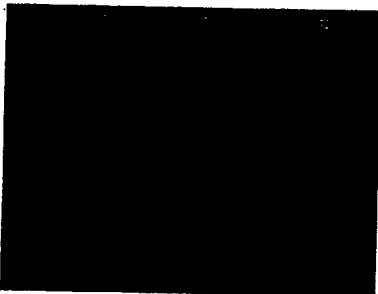


Figure 17 Two Tubes, Pattern 2

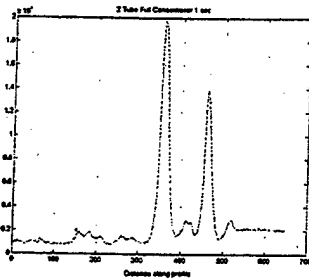


Figure 18 Profile Two Tubes Full Concentrator

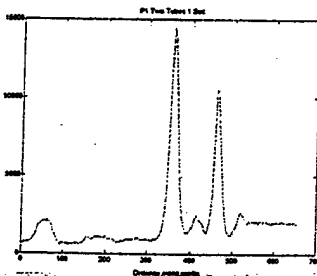


Figure 19 Profile Two Tube Pattern 1

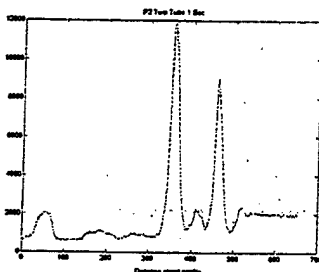


Figure 20 Profile 2 Tube Pattern 2

Conclusions and Future Work:

From the experiments conducted for this paper, the concept of using the cylindrical mirrors of the tubing for the absorber as a Wavefront sensor appears to be feasible and correct. The method of using one tube to look at the concentrator model revealed the fact that the CCD camera being used does not have enough resolution to image the concentrator reflection at 1 meter. The two-tube experiment showed a very promising pattern in that it showed a decrease in intensity in conjunction with a reduction in the white areas from the full concentrator to the other two patterns. Since the patterns did not represent actual misalignment, further work is needed to make suitable patterns to represent misalignment.

Information from the image of the can did not produce an image of the concentrator as expected. Some possible reasons for this anomaly were CCD camera not focused properly for the can, misalignment of the camera, the black areas of the model were not opaque, and a field of view that was too small for the type of image wanted.

Future work will focus on improving the concentrator models by making them conform to actual misalignment and to making the black areas able to block more light. A possible error source in the images may be IR light from the overhead projector getting into the CCD and causing the intensities to depend more on the IR instead of just the white light. Also, since the projector was not completely black around the areas backlit, scattered light may have entered the CCD and cause intensity changes. A quick way to make the black outlines darker and opaque to IR is to either back the model with cardboard or make the patterns out of Aluminum foil.

The concentrator model, to model actual misalignment, would have to be constructed such that the dark areas appear at the edges of the concentrator first as the concentrator moves out of focus. At that point the concentrator would have a white center with black edges. Some modeling and simulation of the concentrator or the use of an actual concentrator may be needed to actually produce and verify this effect.

The copper coiled absorber sensor would become the primary target for images of the concentrator model. An actual 1 X 2 meter concentrator will be available soon to perform more analysis of the image formed in the concentrator when off focus. Finally, a camera with more resolution will be made available to allow more experimentation with the one tube and can to investigate the full image of the concentrator providing more insight to the functioning of the cylindrical mirrors and wave front sensor.

¹ Shack, Roland, Dr., Ben C. Platt, Ph. D., "History and Principles of Shack-Hartmann Wavefront Sensing." Journal of Refractive Surgery, Vol. 17, September/October 2001.

² IBID.